IL NUOVO CIMENTO Vol. 34 C, N. 2 Marzo-Aprile 2011
DOI 10.1393/ncc/i2011-10838-5

Colloquia: WISH2010

# The latest results from the ATLAS experiment

V. Perez-Reale for the ATLAS Collaboration
*Nevis Laboratory, Columbia University - 136 So. Broadway, Irvington, NY 10533, USA*

(ricevuto il 18 Ottobre 2010; approvato il 9 Novembre 2010; pubblicato online il 22 Marzo 2011)

**Summary.** — With the LHC start-up and the first runs at 900 GeV, 2.36 TeV and 7 TeV centre-of-mass energy in the years 2009 and 2010, the ATLAS detector started to record its first collision events. The delivered integrated luminosity has now reached 3.69 $\mathrm{pb}^{-1}$. These data have been used to perform detailed studies on the performance of the detector, including measuring charged and neutral particle mass resonances and the study of QCD cross-sections. The data have already made it possible to commission and calibrate the various ATLAS subdetectors, and understand their performance in detail. The first observation of Standard Model electroweak processes, in particular mass resonances, is also being used as a benchmark for validating the analysis and simulation tools. The status and performance of the detector is briefly reviewed, the latest physics results are summarized and limits on new physics are given.

PACS 29.40.Gx – Tracking and position-sensitive detectors.
PACS 14.70.Fm – $W$ bosons.
PACS 14.70.Hp – $Z$ bosons.
PACS 12.38.-t – Quantum chromodynamics.

## 1. – Introduction

The Large Hadron Collider (LHC) started operation in November 2009 and has delivered proton-proton (p-p) collisions at 0.9 TeV, 2.36 TeV and 7 TeV centre-of-mass energy ($\sqrt{s}$) and delivered an integrated luminosity of 3.69 $\mathrm{pb}^{-1}$. The ATLAS detector has used the data collected to scrutinize the detector performance in detail, discover Standard Model (SM) physics and set new limits on physics beyond the SM at this new energy regime. Some examples of this wide spectrum of physics results will be presented in this report.

## 2. – ATLAS status and LHC environment

The ATLAS detector [1] has several major components. The innermost is composed of silicon pixel, silicon strip and transition radiation tracking detectors covering the pseudo-rapdity region $|\eta| < 2.5$ and immersed in a homogeneous 2 Tesla magnetic field provided

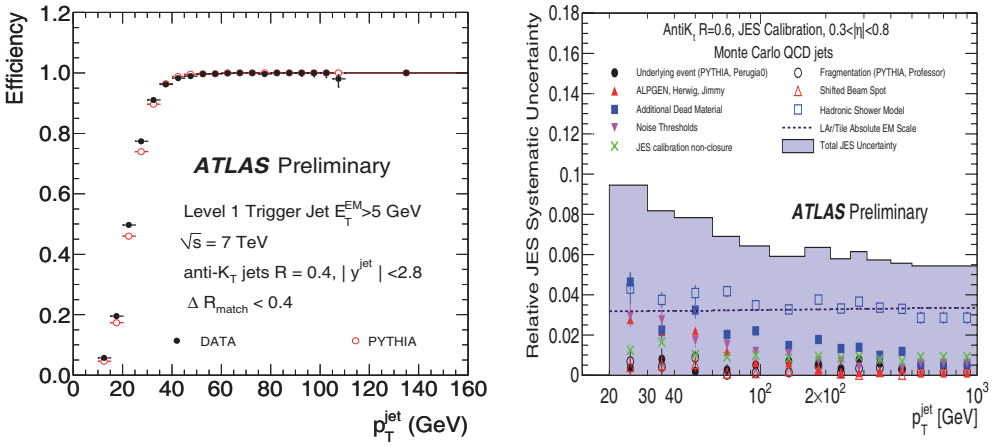


Fig. 1. – (Colour on-line) Level1 trigger efficiency for the lowest jet threshold, $p_T > 5\,\text{GeV}$, as a function of the calibrated offline reconstructed jet object (left). The relative jet energy scale systematic uncertainty as a function of the jet $p_T$ in the pseudorapidity region $0.3 < |\eta| < 0.8$ in the calorimeter barrel. The total uncertainty is shown as the solid light blue area (right).

by a superconducting solenoid. These are surrounded by a hermetic calorimeter that covers $|\eta| < 4.9$ and provides three-dimensional reconstruction of electromagnetic and hadronic particle showers. Outside the calorimeter, there is a muon spectrometer with three air-core toroids providing a non-uniform magnetic field integral averaging about 3 Tesla-m, which provides precision measurements and triggering capability. A hardware-based first level (Level-1) trigger is used to select p-p collisions of interest, and software algorithms are applied to these candidates in a two-stage high-level trigger (HLT) that determines which events are recorded for offline processing. The ATLAS detector has a total of 100 million electronic channels, the non-working fraction does not exceed 2–3%, providing good data quality. Through the end of August 2010 ATLAS recorded $3.46\,\text{pb}^{-1}$ of integrated luminosity with an excellent overall detector data taking efficiency of 95%. The knowledge of the absolute luminosity delivered by the LHC at the ATLAS interaction point is important for cross-section measurements. The instantaneous luminosity was estimated with a combination of independent methods with an uncertainty of 11% [2], dominated by the measurements of beam currents. The peak instantaneous luminosity reached in ATLAS was $L = 1.0 \times 10^{31}\,\text{cm}^{-2}\,\text{s}^{-1}$.

## 3. – ATLAS detector performance

Already with the first LHC p-p collisions, ATLAS devoted a substantial amount of work to understand the detector performance to assure solid physics measurements. In this section, a few examples of ongoing performance studies will be presented.

**3**˙1. *Trigger system.* – A crucial and delicate operation in hadron colliders is the commissioning of the trigger system. The ATLAS three-level trigger system was commissioned adapting to the constant increase in instantaneous luminosity to have the highest acceptance to physics. Figure 1 (left) shows the Level-1 trigger efficiency for the lowest jet threshold, transverse momentum $p_T > 5\,\text{GeV}$ at the electromagnetic scale, as

a function of the calibrated offline reconstructed jet object. The data (black dots) agrees well with Pythia [3] Monte Carlo (MC) simulations (red dots). The jet trigger is fully efficient at an offline transverse momentum threshold of 40 GeV [4].

**3**˙2. *Tracking*. – A very important measurement is the mapping of the Inner Detector material. There are several methods to map the material, reconstruction of the conversion point in the radial direction of photon conversions, $K_s$ decays [5, 6]. The Inner Detector material is presently known to $\sim 10\%$, the goal is to known the material to $\sim 5\%$ for W boson mass reconstruction. From first measurements of early $K_s$ decays and $J/\psi$ to two electrons we were able to conclude that in the low momentum $p_T$ region the momentum scale is known to the per mil level and resolution is dominated by multiple scattering as expected.

**3**˙3. *Missing energy and jets*. – Missing energy is sensitive to calorimeter performance (dead cells, mis-calibrations) and cosmic rays and beam induced backgrounds. backgrounds. Good agreement between the calibrated transverse missing energy in minimum bias data compared to MC samples has been observed for the full rapidity region $|\eta| < 4.9$ [7], after removal of non-collision backgrounds.

Understanding and measuring the performance of jets is crucial for the understanding of physics at LHC: a correct estimate of the energy of jets (jet energy scale, or JES) is input to many physics analyses, and its uncertainty is the dominant experimental uncertainty for measurements such as the di-jet cross-section, the top quark mass measurements and new physics searches with jets in the final state. The energy scale of jets measured in the ATLAS calorimeters [8] is calibrated on average to the hadronic scale using simulated MC QCD jets samples. This MC simulation has been validated with data collected by the ATLAS detector at $\sqrt{s} = 0.9\,\text{TeV}$ and $\sqrt{s} = 7\,\text{TeV}$. The energy contribution of multiple p-p interactions to calorimeter jets is not accounted for in the current JES calibration; it is included as a separate contribution to the systematic uncertainty, and it is shown to contribute less than 2%. The JES systematic uncertainty is evaluated by comparing the nominal results to MC simulations using alternative detector configurations, alternative hadronic shower and physics models, and by comparing the response of jets in data and simulation over the entire range of pseudorapidity. Figure 1 (right) shows the relative jet energy scale systematic uncertainty as a function of the jet $p_T$ in the pseudorapidity region $0.3 < |\eta| < 0.8$ in the calorimeter barrel. Jets have been reconstructed using the jet clustering anti-$k_T$ algorithm [9]. The total uncertainty is shown as the solid light blue area. The individual sources are also shown, with statistical errors. The calorimeter contribution to the JES uncertainty is verified with a method that propagates the uncertainties on the single particle energy deposits comprising the jets. This estimate is based on single particle studies using collision data and test beam measurements. For inclusive jets with $p_T > 20\,\text{GeV}$ and pseudorapidity smaller than 2.8, the jet energy scale is determined with an uncertainty smaller than 10%. The uncertainty will be reduced to a few percent once more statistics on photon-jet events are collected and *in situ* measurements of the JES with data can be performed.

**3**˙4. *Electrons and muons*. – The early performance studies of the inner tracker, calorimeter and muon system were possible thanks to the reconstruction of resonances [10]. The di-muon invariant mass spectrum for data, from opposite sign muons in triggered events is shown in fig. 2 (left) for an integrated luminosity of $0.9\,\text{pb}^{-1}$. The muon trigger applies a $p_T$ threshold at 6 GeV, while the two inner detector-muon spectrometer combined tracks have a $p_T$ threshold of 4 and 2.5 GeV, respectively. Figure 2

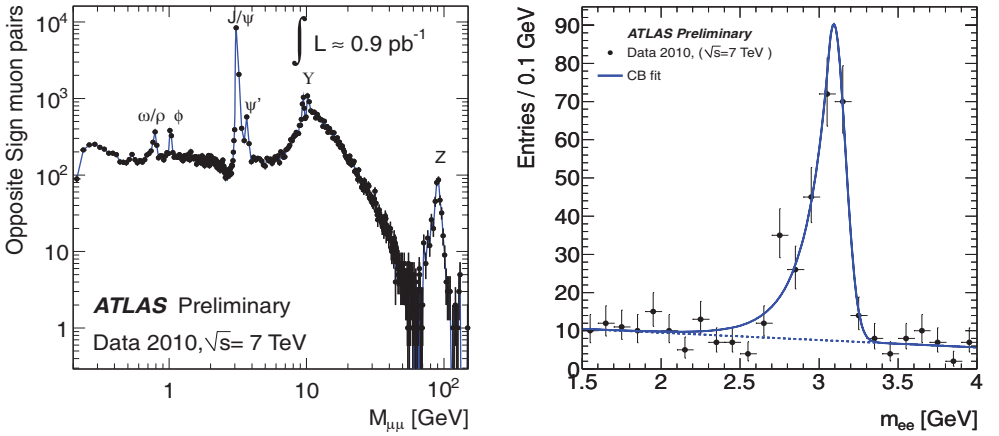


Fig. 2. – Di-muon invariant mass spectrum for data, from fully combined opposite sign muons (left). Invariant mass spectrum for opposite sign electrons (right).

(right) shows the invariant mass of the $J/\psi \to e^+e^-$ calculated for an integrated luminosity of $78\,\mathrm{nb}^{-1}$. The signal is the integration of a fit from 1.5 to 4 GeV and the background (dashed blue) is the integration of a fit result for an invariant mass of $M - 3\sigma$ to $M + 2\sigma$. The mass peak $(3.09 \pm 0.01)$ GeV is in good agreement with MC expectations.

## 4. – QCD physics

**4˙1.** *Minimum bias.* – The first ATLAS physics measurement published was the charged particle distributions at $\sqrt{s} = 0.9\,\mathrm{TeV}$ [11]. Charged particles within the kinematic phase space of $p_T > 500\,\mathrm{MeV}$, $|\eta| < 2.5$, and $N_{\mathrm{ch}} \geq 1$ where $p_T$ is the momentum of the particle in the direction transverse to the beam, $N_{\mathrm{ch}}$ is the number of charged particles in an event, were studied. Charged-particle multiplicity measurements were then performed using the first $\sqrt{s} = 7\,\mathrm{TeV}$ collisions delivered by the LHC during 2010, for the same $p_T$ range and in addition for a phase-space of $p_T > 100\,\mathrm{MeV}$ and $|\eta| < 2.5$. Based on over ten million p-p inelastic interactions, the properties of events with at least two primary charged particles produced were studied for the latter kinematic region [12]. The results have had detector effects unfolded so that they can be compared to particle-level calculations. The charged-particle multiplicity per event and unit of pseudorapidity at $|\eta| = 0$ was measured to be $\mathrm{d}N_{\mathrm{ch}}/\mathrm{d}\eta = 5.635 \pm 0.002(\mathrm{stat.}) \pm 0.149(\mathrm{syst.})$ at 7 TeV and $\mathrm{d}N_{\mathrm{ch}}/\mathrm{d}\eta = 3.486 \pm 0.008(\mathrm{stat.}) \pm 0.077(\mathrm{syst.})$ at 0.9 TeV. The charge particle distributions as a function of rapidity are larger than all MC predictions within 20–30%, the data are very precise with an experimental error less than a few percent. Recently measurements were performed in a diffractive limited phase space, using a cut on $N_{\mathrm{ch}}$ at six particles per event, and a new minimum bias tune, AMBT1 [13], was produced using those results for the first $190\,\mu\mathrm{b}^{-1}$ of data. The average charged particle multiplicity per unit of rapidity for $|\eta| = 0$ as a function of the $\sqrt{s}$ is shown in fig. 3 (left). The results with $N_{\mathrm{ch}} \geq 2$ within the kinematic range $p_T > 100\,\mathrm{MeV}$ and $|\eta| < 2.5$ are shown alongside the results with $N_{\mathrm{ch}} \geq 1$ within the kinematic range $p_T > 500\,\mathrm{MeV}$ and $|\eta| < 2.5$ at $\sqrt{s}$ 0.9, 2.36 and 7 TeV. The data are compared to various particle level MC predictions. The MC describes the data worse for $p_T > 100\,\mathrm{MeV}$ than for $p_T > 500\,\mathrm{MeV}$; some of

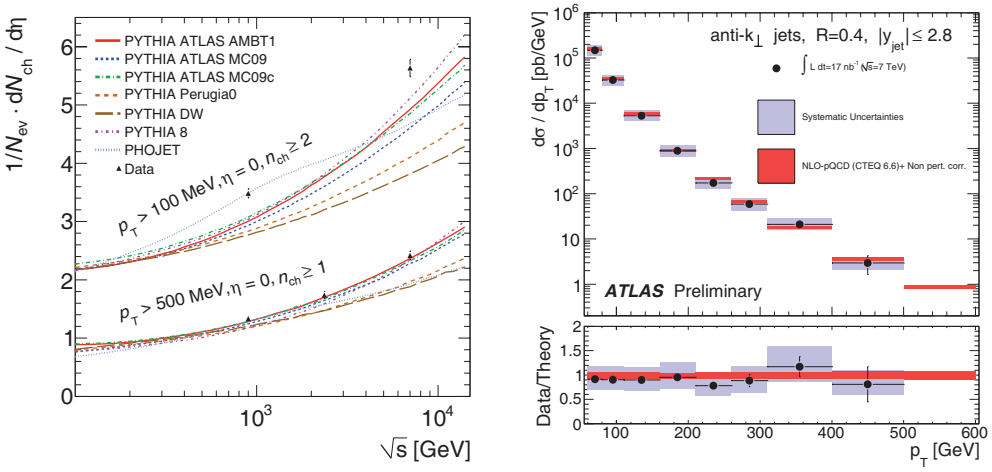


Fig. 3. – (Colour on-line) The average charged particle multiplicity per unit of rapidity for $|\eta| = 0$ as a function of the $\sqrt{s}$ energy (left). The inclusive jet differential cross-section as a function of the jet $p_T$ integrated over the full region $|y| < 2.8$ for jets identified using the anti-$k_T$ algorithm with $R = 0.4$ (right).

this can be attributed to the larger contribution from the diffractive components. The best agreement for the kinematic range $p_T > 500\,\text{MeV}$ is given by the new minimum bias tune, AMBT1.

**4˙2.** *Inclusive jet measurements.* – Jet rates and cross-sections are key observables in high-energy particle physics. They have been measured in different colliders with different probes. Jet cross-sections have been measured with the ATLAS detector for the first time in p-p collisions at $\sqrt{s} = 7\,\text{TeV}$, using an integrated luminosity of $17\,\text{nb}^{-1}$ [14]. The anti-$k_T$ algorithm has been used to identify jets, using two jet radius parameters, $R = 0.4$ and 0.6. The cross-sections were extended up to a jet $p_T$ of 500 GeV and dijet masses of 2 TeV. The leading logarithmic parton-shower MC was found to provide a reasonable description of the energy flow around the jets and of the shapes of the cross-sections. The inclusive jet differential cross-section as a function of jet $p_T$ integrated over the full region $|y| < 2.8$ for jets identified using the anti-$k_T$ algorithm with $R = 0.4$ is shown in fig. 3 (right). The data are compared to NLO QCD calculations to which soft QCD corrections have been applied. The error bars indicate the statistical uncertainty on the measurement, and the grey shaded band indicates the quadratic sum of the systematic uncertainties, dominated by the jet energy scale uncertainty. The luminosity uncertainty is not shown. The theory uncertainty shown in orange is the quadratic sum of uncertainties from the choice of renormalisation and factorisation scales, parton distribution functions, $\alpha_s(M_Z)$, and the modelling of soft QCD effects. The measurements were found to be well described by fixed-order NLO perturbative QCD calculations.

## 5. – First observations of W and Z bosons

The $W^{\pm}$ and Z bosons are expected to be produced abundantly at the LHC, and for the first time in p-p collisions. The well-known properties of these bosons will provide significant constraints in the determination of the ATLAS detector performance,

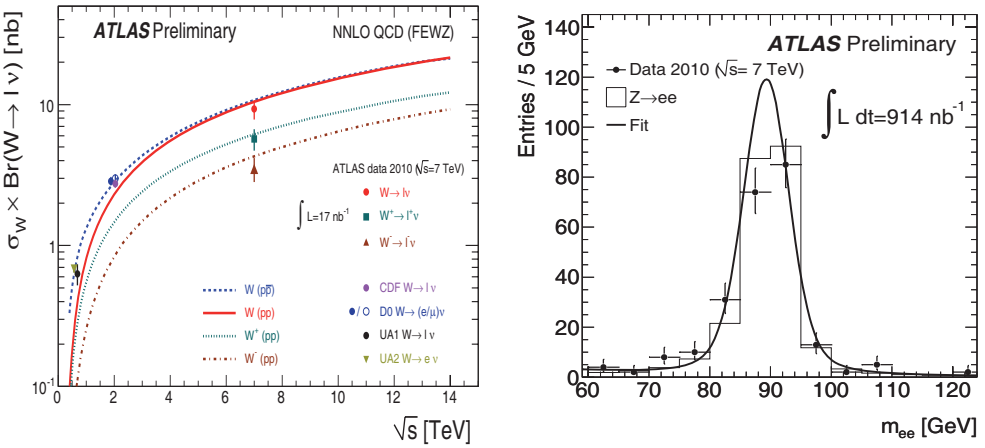


Fig. 4. – The measured values of sigma of $W \times BR(W \to l\nu)$ for $W^+$ and $W^-$ and for their sum compared to the theoretical predictions based on NNLO QCD calculations (left). The invariant mass distribution of the opposite-charged Z candidate electrons (right).

powerful tools to constrain parton distribution functions (PDF's) inside the proton and understanding for search of new physics for which these processes are backgrounds.

**5˙1.** *W bosons.* – The ATLAS experiment observed 3233 $W \to e\nu$ and 3425 $W \to \mu\nu$ candidates [15] produced from the $\sqrt{s} = 7\,\text{TeV}$ p-p collisions of the LHC, resulting from a total integrated luminosity of $1.01\,\text{pb}^{-1}$ and $991\,\text{nb}^{-1}$, respectively. The analysis requires well-reconstructed and isolated leptons with high transverse momentum combined with missing transverse energy of 25 GeV. The QCD component of the background is estimated from data, while the electroweak component is obtained from MC. The W bosons cross-sections were measured in 7 TeV p-p collisions for a total integrated luminosity of $17\,\text{nb}^{-1}$ [16]. The total inclusive W-boson production cross-section times the leptonic branching ratio is measured to be $8.5 \pm 1.3(\text{stat.}) \pm 0.7(\text{syst.}) \pm 0.9(\text{lumi.})\,\text{nb}$ for the $W \to e\nu$ channel and $10.3 \pm 1.3(\text{stat.}) \pm 0.8(\text{syst.}) \pm 1.1(\text{lumi.})\,\text{nb}$ for the $W \to \mu\nu$ channel. The result obtained is in agreement with theoretical calculations based on NNLO QCD. In addition the expected charge asymmetry between the cross-sections for $W^+$ and $W^-$ production has been experimentally confirmed. The measured values of production cross-sections of $W \times BR(W \to l\nu)$ for $W^+$ and $W^-$ and for their sum compared to the theoretical predictions based on NNLO QCD calculations are shown in fig. 4 (left). Results are shown for the combined electron-muon results. The predictions are shown for both p-p ($W^+$, $W^-$ and their sum) and proton-antiproton colliders W as a function of $\sqrt{s}$. The calculations are based on the FEWZ program [17] with the MSTW2008 NNLO [18] structure function parameterisations. In addition, measurements at previous proton-antiproton colliders are shown. The data points at the various energies are staggered to improved readability. The data points are plotted with their total uncertainty.

**5˙2.** *Z bosons.* – For the Z boson channel, datasets of $914\,\text{nb}^{-1}$ and $1.07\,\text{pb}^{-1}$ were used for the analysis, leading to 230 and 354 Z bosons candidates in the invariant mass window of (66–116) GeV, for the electron and muon channels, respectively. In the electron channel [19], pairs are formed from oppositely-charged electron-positron candidates.

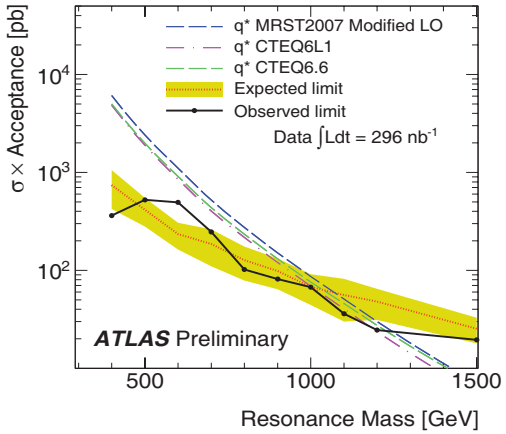


Fig. 5. – (Colour on-line) The 95% CL upper limits on $\sigma \cdot \mathcal{A}$ as a function of the di-jet resonance mass $m^{jj}$ (dots) is shown on the left, expected 95% CL upper limit (red dotted), and excited quarks $\sigma \cdot \mathcal{A}$ predictions for different MC tunes (dashed).

These electron candidates are required to have a cluster transverse energy $E_T > 20\,\text{GeV}$ within $|\eta| < 2.47$, excluding the region between the barrel and end-cap calorimeters ($1.37 < |\eta| < 1.52$). The invariant mass distribution of the opposite-charged Z candidate electrons is shown in fig. 4 (right) and a fit is superposed to these data. The data are modelled using the theoretical lineshape, including photon and Z contributions, convolved with a Gaussian resolution function. The fitted peak of the distribution is found to be $90.9 \pm 0.3\,\text{GeV}$ (91.6 GeV from the MC). The experimental resolution is found to be $3.2 \pm 0.3\,\text{GeV}$ (1.8 GeV from the MC). The discrepancy between the experimental resolution from the data fits compared to MC will be reduced with improvements in the electromagnetic calibration. The total inclusive Z-boson production cross-section times the charged leptonic branching ratio within the invariant mass window $66 < m_{ee} < 116\,\text{GeV}$ was measured in $225\,\text{nb}^{-1}$ to be $0.83 \pm 0.07(\text{stat.}) \pm 0.06(\text{syst.}) \pm 0.09(\text{lumi.})\,\text{nb}$. Within the experimental uncertainties, the measured cross-section agrees well with the NNLO QCD calculation $(0.964 \pm 0.03)\,\text{nb}$.

## 6. – Physics beyond the SM

**6˙1.** *Excited quarks.* – Several extensions of physics beyond the SM predict new heavy particles, accessible at LHC energies, that decay into two energetic partons. Such new states may include an excited composite quark q*. A search for new heavy particles manifested as narrow resonances in two-jet final states [20] was performed with the data collected by the ATLAS detector, produced in $\sqrt{s} = 7\,\text{TeV}$ p-p collisions, which correspond to an integrated luminosity of $315\,\text{nb}^{-1}$. The analysis technique consisted in the search for a di-jet mass resonance $m^{jj}$ on top of a smooth and rapidly falling spectrum and relied on the measured $m^{jj}$ distribution to estimate the background level to this new possible signal. Events with two jets computed via the anti-$k_T$ algorithm with a radius $R = 0.6$ were retained if the highest $p_T$ jet satisfied $p_T^j > 80\,\text{GeV}$ and the next to leading jet $p_T^j > 30\,\text{GeV}$ and both jets be in $|\eta^j| < 2.5$ with their pseudorapidity difference

$|\eta^{j1} - \eta^{j2}| < 1.3$. The final event sample was selected by requiring $m^{jj} > 200\,\text{GeV}$. No resonances were observed. Upper limits were set (using a Bayesian approach) on the product of cross-section $\sigma$ and detector acceptance $\mathcal{A}$ for excited-quark ($\text{q}^*$) production as a function of $\text{q}^*$ mass. These exclude at the 95% credibility-level (CL) the $\text{q}^*$ mass interval $0.40 < m^*_{\text{q}} < 1.26\,\text{TeV}$ using MRST2007 [21] PDFs in the ATLAS default MC09 tune, extending the reach of previous experiments. Figure 5 depicts the resulting 95% CL upper limits on $\sigma \cdot \mathcal{A}$ as a function of the $\text{q}^*$ resonance mass. The red dotted curve shows the expected 95% CL upper limit of $\sigma \cdot \mathcal{A}$ as a function of the dijet mass $m^{jj}$. The yellow band represents the RMS of the limit due to Poisson fluctuations of the pseudo-data around the LO Pythia QCD prediction. The corresponding observed limit is shown by the black solid curve. The dashed curves represent excited-quark $\sigma \cdot \mathcal{A}$ predictions for different PDF scenarios. The expected and observed limits are shown with all systematic uncertainties included.

## 7. – Conclusions

The LHC has produced record energy collisions since March 2010. Since then the ATLAS detector has promptly delivered high-quality results covering a wide spectrum of physics processes. With the $3.46\,\text{pb}^{-1}$ integrated luminosity collected, ATLAS has scrutinized the detector performance, reconstructed stable objects and resonances, and entered the TeV scale regime of jet physics. In addition, several hundreds Z bosons and thousands of W bosons decaying to leptons have been recorded, and several top quark event candidates have been observed. The era of physics searches beyond the SM has started, ATLAS has extended the current world limits on excited quark production and many other searches are ongoing.

REFERENCES

[1] Aad G. *et al.* (ATLAS Collaboration), *JINST*, **3** (2008) S08003.
[2] Aad G. *et al.* (ATLAS Collaboration), ATL-CONF-2010-060 (2010).
[3] Sjostrand T., Mrenna S. and Skands P. Z., *JHEP*, **0605** (2006) 21.
[4] Aad G. *et al.* (ATLAS Collaboration), ATL-CONF-2010-050 (2010).
[5] Aad G. *et al.* (ATLAS Collaboration), ATL-CONF-2010-019 (2010).
[6] Aad G. *et al.* (ATLAS Collaboration), ATL-CONF-2010-058 (2010).
[7] Aad G. *et al.* (ATLAS Collaboration), ATL-CONF-2010-057 (2010).
[8] Aad G. *et al.* (ATLAS Collaboration), ATL-CONF-2010-056 (2010).
[9] Cacciari S. G. P. and Soyez G., *JHEP*, **04** (2008) 063.
[10] Aad G. *et al.* (ATLAS Collaboration), ATL-CONF-2010-078 (2010).
[11] Aad G. *et al.* (ATLAS Collaboration), *Phys. Lett. B*, **688** (2010) 21.
[12] Aad G. *et al.* (ATLAS Collaboration), ATL-CONF-2010-046 (2010).
[13] Aad G. *et al.* (ATLAS Collaboration), ATL-CONF-2010-031 (2010).
[14] Aad G. *et al.* (ATLAS Collaboration), arXiv:1009.5908 [hep-ex] (2010).
[15] Aad G. *et al.* (ATLAS Collaboration), ATL-COM-PHYS-2010-551 (2010).
[16] Aad G. *et al.* (ATLAS Collaboration), ATL-CONF-2010-051 (2010).
[17] Anastasiou C., Dixon L., Melnikov K. and Petriello F., *Phys. Rev. D*, **69** (2004) 094008.
[18] Martin A. D., Stirling W. J., Thorne R. S. and Watt G., *Phys. J. C*, **63** (2009) 189.
[19] Aad G. *et al.* (ATLAS Collaboration), ATL-CONF-2010-076 (2010).
[20] Aad G. *et al.* (ATLAS Collaboration), arXiv:1008.2461v1 [hep-ex] (2010).
[21] Shersnev A. and Thorne R. S., *Eur. Phys. J. C*, **55** (2008) 553.